

# Genome-Wide Identification Of Hydrocarbon Degradation Pathways In *Bacillus Paralicheniformis* Using KEGG And Docking Integration

Srimathi Murugesan<sup>1</sup>, Abirami Gopalakrishnan<sup>2</sup>

<sup>1,2</sup>Department of Biotechnology, School of Life Sciences, Vels Institute of Science Technology and Advanced Studies, Pallavaram, Chennai, Tamil Nadu, India

\*Corresponding author: Abirami G; [drabirami.cas@gmail.com](mailto:drabirami.cas@gmail.com)

---

## Abstract

Specific bacteria and fungi are linked to the oxidative breakdown of hydrocarbons and their derivatives in soil and water contaminated by crude oil spills in these habitats. The binding affinity of hydrocarbons and their derivatives in a crude oil sample to the cysteine dioxygenase of *Bacillus subtilis* was examined by computational approaches. The study attempted to validate the assertion of the effective utilization of this organism in crude oil cleanup and to ascertain the selectivity of the chemicals in the crude by this bacterial enzyme. The constituents of the analysed crude oil sample were determined using gas chromatography-mass spectrometry. The crude oil sample was found to contain 47.48% monomers and 52.52% derivatives, with hydrocarbons comprising 29.44% straight-chain, 13.79% branch-chain, and 4.25% cyclic molecules. Notably, the hydrocarbons included 22.83% ketones, 1.72% alcohol, and 27.97% carboxylic acids. Binding interactions with the protein target were characterized, revealing that all drugs bound outside the active sites, primarily through hydrogen, alkyl, van der Waals, pi-alkyl, and pi-sigma interactions. The binding free energy values indicated that decane, dodecane, and eicosane exhibited the highest binding free energy (-2.9 kcal/mol), suggesting weak affinity for the protein and impractical oxidation by the enzyme. Docking scores for various hydrocarbons were assessed, with significant interactions noted at specific protein sites, particularly with residues LYS27, ALA32, ALA33, and MET85. The study highlights that certain hydrocarbons, particularly cyclic and branched structures, are more susceptible to oxidation by *Bacillus Paralicheniformis*, indicating potential for effective bioremediation in crude oil-contaminated environments.

**Key words:** Molecular docking, *Bacillus paralicheniformis*, Alcohol dehydrogenase, Babel GUI, PyMOL.

---

## INTRODUCTION

Oil Spills refer to unregulated discharges of any substance, notably crude oil, chemicals, or garbage, into the environment. It is typically attributable to equipment malfunction, operational errors, human mistakes, or deliberate harm to infrastructure [1]. The degree of harm is contingent upon the nature, location, volume of the spill, and the duration of its presence in the affected ecosystem [2]. An oil spill refers to the discharge of liquid petroleum hydrocarbons into the environment, particularly affecting marine ecosystems [3]. Upon the release of oil, less volatile and denser fractions remain, whereas lighter fractions evaporate. Oil spills typically lead to the mortality of aquatic and terrestrial fauna, while also depriving the indigenous human population of their food sources and livelihoods [4] [5].

The remediation of oil spill sites is arduous and can require months or even years to complete. Various oil cleanup techniques, including hot water and high-pressure washing, dispersants, sorbents, skimmers, oil booms, and bioremediation, are presently employed [6]. Bioremediation, which employs native or introduced oil-degrading microbes or other living forms to decompose various constituents of spilled petroleum in marine environments, has emerged as a promising invention due to its little effort and environmentally beneficial characteristics [7,8]. This technology enables the safe, cost-effective, and more efficient cleanup of oil spills compared to alternative physical or chemical techniques. Bioremediation primarily operates by biodegradation, which entails the total mineralization of organic pollutants into carbon dioxide, water, inorganic substances, and cellular proteins [9]. Multiple studies have revealed a vast array of hydrocarbon-degrading microbes in oil-rich environments, such as oil spill sites and oil reservoirs, with their prevalence influenced by the specific types of petroleum hydrocarbons and surrounding environmental circumstances [10-15]. Among these organisms are *Pseudomonas fluorescens*, *P. aeruginosa*, *Bacillus subtilis*, *Bacillus* sp., *Alcaligenes* sp., *Acinetobacter lwoffii*, *Flavobacterium* sp., *Micrococcus roseus*, and *Corynebacterium* sp [16]. The genus *Bacillus* has been reported to be an outstanding hydrocarbon degrader, and their ability to form spores when nutrients are limited makes

them self-sustainable bioremediation organisms [17]. It has been demonstrated that the processes that lead to degradation of a variety of petroleum hydrocarbons involve oxidizing responses; however, these pathways exhibit substantial variations due to the distinct oxygenase present in different bacterial species. For example, certain microbes are capable of metabolizing particular alkanes, while others, such as *Proteus vulgaris* and *Proteus cibarius*, degrade aromatic or resin fractions of hydrocarbons [18]. Specific disciplines are studied through the use of computer hardware, software, and networking tools in computer-aided learning. The utilization of computer algorithms in the biodeterioration of crude oil-polluted habitats would provide direct insight into the organisms that are most appropriate for the remediation of a specific crude oil pollution site, as microbial enzymes selectively degrade crude oil polymers. The time and cost associated with direct trials of these microbes on polluted sites could be reduced by utilizing in silico methods to initially identify the appropriate microorganisms for the degradation of crude oil of a specific hydrocarbon composition. This paper conducted a computer-guided degradation susceptibility investigation of crude oil substances on the enzyme of the *Bacillus Paralicheniformis* protein target. The findings would confirm the reports regarding the efficacy of this entity in facilitating the breakdown of crude oil and could pinpoint the hydrocarbons that are most susceptible to deterioration by its enzyme.

## MATERIALS AND METHOD

### Collection of crude oil and bilge water from the bilge tank of a ship

Collection of 500ml of crude oil and one liter of bilge water from a private passenger ship at Chennai Sea Port, India. The sample collection was conducted using amber glass vials with Teflon-lined lids. In order to prevent evaporative modifications and microbial breakdown in the crude oil during transport to the laboratory, the collected samples were sealed and labelled before being stored in a dark, insulated refrigerator. The samples were subjected to gas chromatography evaluation on the same day as their collection.

### Examination of Crude Oil Sample

The compounds found in the crude oil sample were identified using Gas Chromatography-Mass Spectrometry (GCMS-QP2010 PLUS, Shimadzu, Japan). A standard internal solution was made from aliquots of the original compounds and diluted with dichloromethane to a final concentration of 0.5 mg/mL. The reference solution contained n-C3 to n-C44. Fig. S1 illustrates the chromatogram of the standard calibration solutions. The calibration curve, limit of detection (LOD), and limit of quantification (LOQ) were all determined for testing the instrument. Five levels of calibration solutions, ranging from 0.02 mg/mL to 1 mg/mL, are generated and utilized to generate a calibration curve by diluting certified solutions containing n-C3 to n-C44. A quadruplicate blank analysis was conducted to ascertain the LOD and LOQ. The LOD indicates when the signal exceeds threefold the smallest quantity of the biomarker. The gradient of the curve used for calibration is denoted by  $S$ , and the standard deviate of the blank test is denoted as  $\sigma$ . The limit of detection (LOD) and limit of quantification (LOQ) were 1.42 and 4.73 mg/mL, respectively. The crude oil traces were analysed subsequent to calibration. The sample syringe has been washed on four occasions with the pre-solvent, four times with the post-solvent, and three more times with the sample. The GC was operated under the following conditions: a carrier gas of helium (1.4 mL/min) and a temperature of 300 °C for the injector and detector. The temperature program consisted of a 0-minute period at 90 °C, followed by a 6 °C/min ramp to 270 °C, and a 30-minute hold at this temperature. 1  $\mu$ L of a 2% volume solution in tetrachloromethane was injected [19].

### Identification and Preparation of Ligands

The 3D structure-data files (SDF) of the chemicals in the crude oil sample were located and retrieved from the PubChem repository. They reduced the size using the PyRx simulator tool. Their minimization was conducted in the PyRx simulation tool utilizing the Universal Force Field over 200 stages. The compounds were subsequently transformed to AutoDock ligands (pdbqt) and utilized for the docking analysis.

### Receptor Preparation

The amino acid sequence of *Bacillus Paralichiniformis*, a candidate Protein selection: RCSB PDB (<https://www.rcsb.org>). Compound database of alcohol dehydrogenase, lipase and esterase: PubChem (<https://pubchem.ncbi.nlm.nih.gov>). Lipinski and ADME studies : SWISSADME (<http://www.swissadme.ch/>), Lipinski rule of five (<http://www.scfbio-iitd.res.in/software/drugdesign/lipinski.jsp>.) with a resolution of 2.30 Å, was found from the literature

[20] and utilized as a target in this investigation. Chain A of the protein was utilized for the docking study to enhance ligand-binding precision [21]. The obstructive crystallographic water ions and co-crystallized ligand were eliminated, followed by energy minimization of the protein utilizing UCSF Chimera 1.14 [22, 23]. The protein was reduced using 300 steepest descent steps at a distance of 0.02 Å. There were 10 conjugate gradient steps at 0.02 Å and 10 update periods. Gasteiger charges were included utilizing Dock Prep to achieve optimal structural conformation. The active sites on the reduced protein (Fig. 1) were found using Biovia Discovery Studio 4.5, created and provided by Dassault Systèmes BIOVIA [24].

### Docking Investigations

The docking of numerous ligands from crude oil molecules onto the protein target was conducted using Autodock Vina in PyRx program version 0.8 [25,26]. Blind docking of the compounds at the protein cavities was conducted to provide the ligands free rein to engage with regions of minimal energy. The central grid box was configured with the following dimensions: center x: -40.037, center y: -18.620, center z: 142.089, and sizes: size x: 50.411, size y: 44.123, size z: 42.859. The binding free energy ( $\Delta G$ ) data for each chemical were obtained.

### Docking Analysis of protein ligand interaction

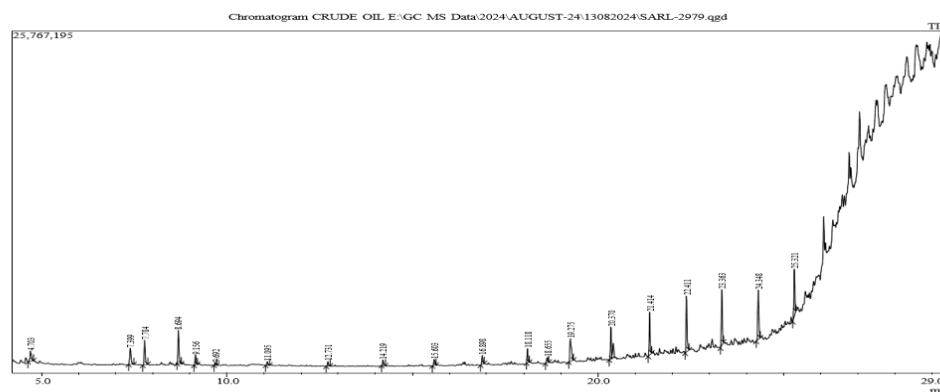
The bonds of hydrogen and other hydrophobic interactions within the protein-ligand structure of the molecules were observed using BabelGUI (software). Followed by AUTODOCK (software), by using DISCOVERY STUDIO VISUALIZER (software), Protein-Ligand Interaction Profiler (<http://plip-tool.biotec.tu-dresden.de>), PyMOL, PDBsum website (<http://www.ebi.ac.uk/thornton-srv/software/PDBsum1/>) analysis is done.

## RESULTS AND DISCUSSION

The chemical components eluted during the gas filtration analysis of the crude oil sample are depicted in Fig. 1. The detected chemicals and their percentage composition in the crude oil sample are presented in Table 1. The sample consisted of 47.48% monomers and 52.52% derivatives of it. The hydrocarbons consisted of 29.44% straight-chain, 13.79% branch-chain, and 4.25% cyclic molecules.

**Fig 1: Gas chromatogram of crude oil sample**

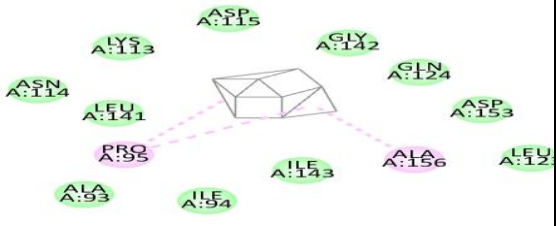
**Table 1: Hydrocarbon and hydrocarbon derivatives of crude oil sample**



6	9.692	9.658	9.733	383933	0.54	194766	0.57	1.97	Mesitylene
7	11.095	11.050	11.158	572698	0.81	279637	0.82	2.05	Undecane
8	12.731	12.683	12.792	672672	0.95	352788	1.04	1.91	Dodecane
9	14.219	14.175	14.283	878454	1.24	434572	1.28	2.02	Pentadecane
10	15.603	15.550	15.650	982112	1.39	464773	1.37	2.11	Tetradecane
11	16.898	16.850	16.950	1384475	1.96	683450	2.01	2.03	Pentadecane
12	18.118	18.092	18.167	1886052	2.67	1056373	3.11	1.79	Nonadecane
13	18.655	18.600	18.700	1050247	1.48	409886	1.21	2.56	Pentadecane, 2,6,10-trimethyl-
14	19.275	19.233	19.358	4950205	7.00	1721275	5.06	2.88	Nonadecane
15	20.370	20.325	20.400	4715987	6.67	2429883	7.15	1.94	Nonadecane, 9-methyl-
16	21.414	21.375	21.475	6228502	8.80	3239193	9.53	1.92	Octadecane
17	22.411	22.375	22.483	8308128	11.74	4210150	12.39	1.97	Heneicosane
18	23.363	23.325	23.408	8309790	11.75	4207111	12.38	1.98	Eicosane
19	24.348	24.292	24.400	7674735	10.85	3714535	10.93	2.07	Docosane
20	25.321	25.275	25.358	6906958	9.76	3511118	10.33	1.97	Heneicosane

The hydrocarbon compounds contained 22.83% ketones, 1.72% alcohol, and 27.97% carboxylic acids. Figure 3 illustrates the binding locations of the hydrocarbon compounds on the protein target. The binding of all drugs transpired outside the protein's active areas. Most chemicals reacted at specified locations on the protein target. The binding free energy values of the substances associated with the protein are presented in Table 2. Table 3 and Table 4. displays the protein-ligand interactions of the docked hydrocarbon molecules. The predominant contact mechanisms between the chemicals and the protein were hydrogen, alkyl, van der Waals, pi-alkyl, and pi-sigma correlations. The majority of oxygen-containing hydrocarbons, along with the control, connected with the proteins through bonding via hydrogen. Alkyl interactions were observed involving the protein and linear hydrocarbons, the majority of which exhibited elevated binding free energies, whereas pi-alkyl interactions predominated among compounds with reduced free energies and the protein.

**Table 2: Protein ligand interaction of crude oil compound and *B. paralicheniformis***

Target gene	Compound	Vanderwaal's interaction	Binding energy (KCal/mol)
	Mesitylene 	ALA 93, ILE 94, ILE 143, LEU 123, ASP 153, GLN 124, GLY 142, ASP 115, LYS 113, ASN 114, LEU 141	-4.67

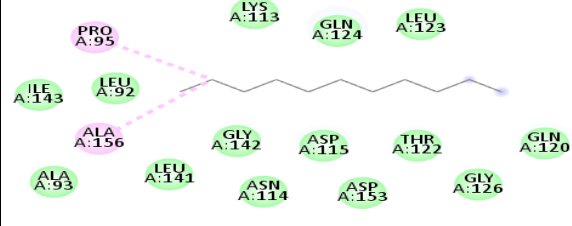
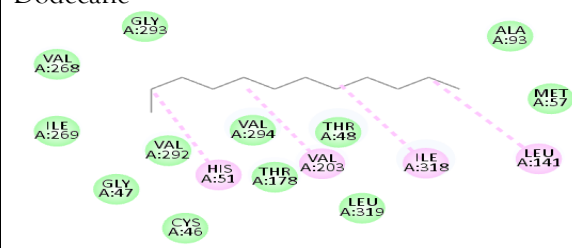
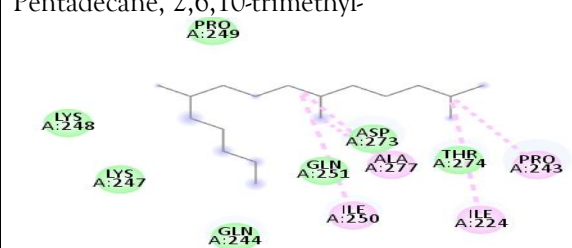
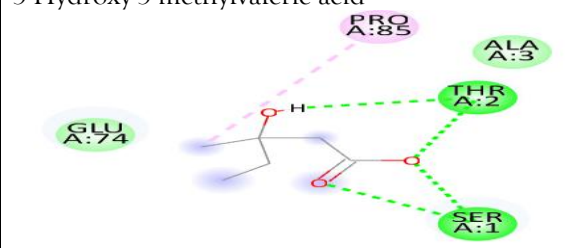
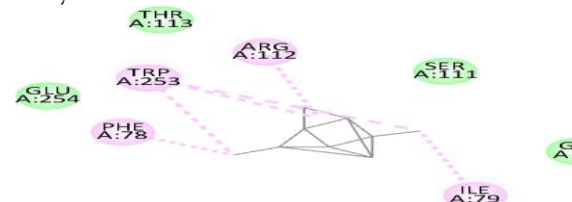
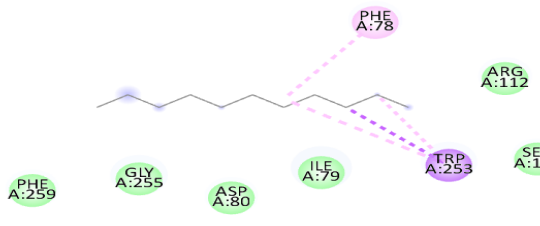
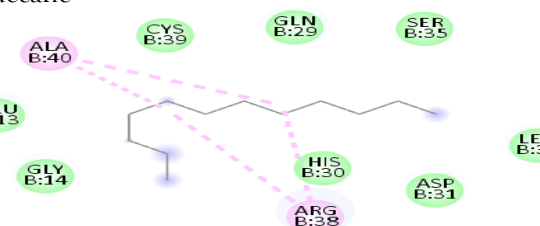
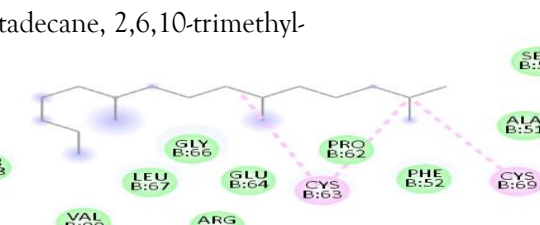
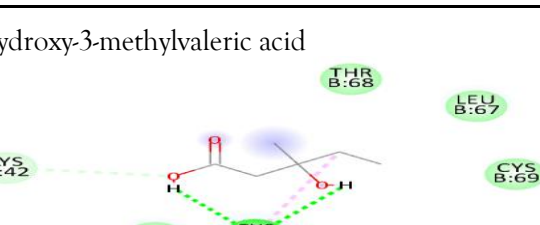
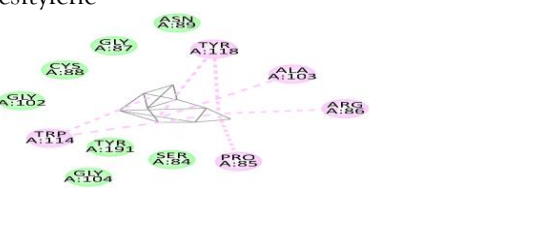
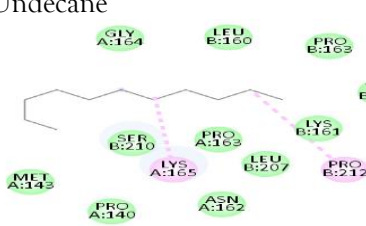
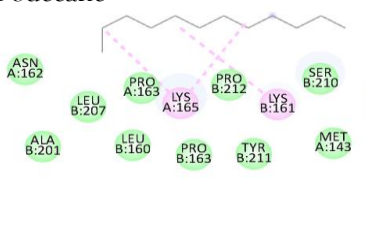
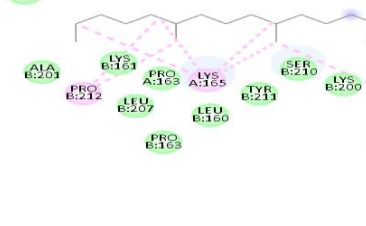
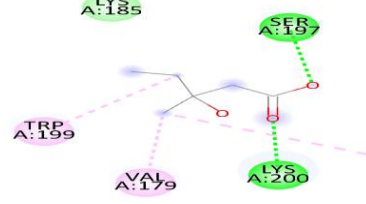
ALCOHOL DEHYDRO GENASE	<p>Undecane</p> 	<p>LYS 113, GLN 124, LEU 123, LEU 92, ILE 143, GLY 142, ASP 115, THR 122, GLN 120, ASP 153, GLY 126, LEU 141, ASN 114, ALA 93</p>	-4.28
	<p>Dodecane</p> 	<p>GLY 293, VAL 268, ALA 93, MET 57, ILE 269, GLY 47, CYS 46, LEU 319, THR 178, THR 48, VAL 294, VAL 292</p>	-3.00
	<p>Pentadecane, 2,6,10-trimethyl-</p> 	<p>PRO 249, LYS 248, LYS 247, GLN 251, GLN 244, ASP 273, THR 274</p>	-2.68
	<p>3-Hydroxy-3-methylvaleric acid</p> 	<p>GLU 74, ALA 3</p>	-2.95

Table.2 Continue

Target gene	Compound	Vanderwaal's interaction	Binding energy (KCal/mol)
	<p>Mesitylene</p> 	<p>GLU 254, THR 113, SER 113, GLY 77</p>	-4.67

LIPASE	<p>Undecane</p> 	<p>PHE 259, GLY 255, ASP 80, ILE 79, SER 111, ARG 112</p>	-4.28
	<p>Dodecane</p> 	<p>GLY 14, GLU 13, CYS 39, GLN 29, SER 35, LEU 36, ASP 31, HIS 30</p>	-3.00
	<p>Pentadecane, 2,6,10-trimethyl-</p> 	<p>THR 68, VAL 90, LEU 67, GLY 66, GLU 64, ARG 65, PRO 62, PHE 52, ALA 51, SER 50</p>	-2.68
	<p>3-Hydroxy-3-methylvaleric acid</p> 	<p>THR 68, LEU 67, CYS 69, GLU 64, PHE 52, PRO 62</p>	-2.95

Target gene	Compound	Vanderwaal's interaction	Binding energy (KCal/mol)
	<p>Mesitylene</p> 	<p>ASN 89, GLY 87, CYS 88, GLY 102, SER 84, TYR 191, GLY 104</p>	-4.52

ESTERASE	<p>Undecane</p> 	<p>MET 143, PRO 140, ASN 162, LEU 207, LYS 167, PRO 163, SER 210, GLY 164, LEU 160, PRO 164, TYR 211</p>	-3.24
	<p>Dodecane</p> 	<p>ASN 162, LEU 207, ALA 201, LEU 160, PRO 163, TYR 211, MET 143, PRO 212, SER 210, PRO 140, GLN 141</p>	-3.34
	<p>Pentadecane, 2,6,10-trimethyl-</p> 	<p>ASN 162, ALA 201, LYS 161, PRO 163, LEU 160, TYR 211, SER 210, LYS 200, GLN 141, LYS 206</p>	-3.51
	<p>3-Hydroxy-3-methylvaleric acid</p> 	<p>LYS 185</p>	-3.42

The amount of binding free energy is the total of all interactions between a ligand and its target. The docking score is the evaluative measure that forecasts the binding affinity between the ligand and target post-docking. The binding free energy of the co-crystallized ligand cysteine (−3.6 kcal/mol) served as a reference norm when assessing the susceptibility of the hydrocarbons to oxidation by the protein [27, 28]. The binding free energy of decane, dodecane, and eicosane was identical (−2.9 kcal/mol) and the highest among all the chemicals examined. The elevated binding free energy values for these chemicals indicate that their affinity for the protein is comparatively weak. Consequently, their oxidation by the protein enzyme would be impractical.

The chemicals docked at analogous sites on the protein of Alcohol dehydrogenase of mesitylene, undecane, dodecane, pentadecane, 2,6,10 trimethyl and 3-Hydroxy-3-met-hylravaleric acid is found to be -4.67, -4.28, -3.00, -2.68 and -2.95 (KCal/mol). The chemicals docked at analogous sites on the protein lipase of mesitylene, undecane, dodecane, pentadecane is found to be -4.19, -3.18, -2.95, -2.89 and -2.29 (KCal/mol). The chemicals docked at analogous sites on the protein esterase of mesitylene, undecane, dodecane, pentadecane is found to be -4.52, -3.24, -3.34, -3.51, -3.42 (KCal/mol).

The chemicals docked at analogous sites on the protein, interacting with LYS27, ALA32, ALA33, and MET85. Tetradecane and nonadecane-2-methyl had identical binding free energy values of  $-3.1$  kcal/mol, being the subsequent highest set recorded. Their dock score indicated that the protein enzyme would inadequately oxidize them. Their interaction transpired at a comparable position, and both substances engaged with LYS34. The binding free energy readings for 2-pentanone 3-methyl- and 1,9-tetradecadiene were identical ( $-3.3$  kcal/mol), while their binding locations on the protein differed. The binding affinities of octane, 2,4,6-trimethyltridecane, hexadecane, n-hexadecanoic acid, octadecane, (Z)-9-octadecenoic acid, and n-octadecanoic acid ( $-3.4$  kcal/mol) were identical, although their interactions with the protein took place at distinct places. The protein's oxidation of these chemicals would likewise be comparatively ineffective, as evidenced by their binding affinities.

The binding free energy values of 2-heptanone 4-methyl-, 4-heptanol 4-methyl-, tetracosane, and 2-pentanone 4-hydroxy-4-methyl- were around  $-3.5$  kcal/mol,  $-3.6$  kcal/mol,  $-3.6$  kcal/mol, and  $-3.7$  kcal/mol, respectively. The median docking scores suggest a high likelihood of oxidation by the protein. The binding of 4-heptanol 3-methyl- and 2-pentanone 4-hydroxy-4-methyl- transpired at the identical location, interacting with ALA32, ALA33, and MET85. The interaction of 2-heptanone-4-methyl- and tetracosane transpired at distinct locations on the peptide. These chemicals comprised 12.52% of the examined crude oil.

The interaction free energies of naphthalene decahydrod-2,6-dimethyl-, methylene cyclododecanone, decane 2,3,5,8-tetramethyl-, 1H-indene octahydro 2,2,4,4,7,7-hexamethyl-trans-, pentadecane 2,6,10-trimethyl-, and pentadecane 2,6,10,14-tetramethyl- were  $-4.8$  kcal/mol,  $-4.8$  kcal/mol,  $-3.8$  kcal/mol,  $-5.1$  kcal/mol,  $-3.8$  kcal/mol, and  $-4.0$  kcal/mol, accordingly, indicating relatively favourable interactions. The binding of naphthalene decahydro 2,6-dimethyl- and 1H-indene octahydro-2,2,4,4,7,7-hexamethyl-trans occurred at the identical location, interacting with TYR4. Methylene cyclododecanone, decane 2,3,5,8-tetramethyl-, and pentadecane 2,6,10-trimethyl- exhibited binding at the identical location and interacted with TYR109. The binding of pentadecane 2,6,10,14-tetramethyl- transpired in a pocket distinct from all other molecules in this categorization, interacting with the residues TYR46 and ALA47. These chemicals comprised 15.39% of the examined crude oil and are either cyclic or extensively branched.

These data indicated that molecules of this structural type are more prone to oxidation by *Bacillus paralicheniformis* and would be effectively remediated in environments contaminated by crude oil.

## CONCLUSION

The selectivity of hydrocarbons in crude oil by the enzyme from *Bacillus paralicheniformis* was investigated in silico. The crude oil sample utilized in the investigation comprised 47.48% hydrocarbons and 52.52% hydrocarbon derivatives. The binding free energy values of the substances on the protein target suggest that the majority of alkanes are resistant to oxidation by the bacterial enzyme, as evidenced by their elevated binding energy of  $-2.9$  kcal/mol. In contrast, poly-branched and cyclic hydrocarbons, exhibiting binding energies between  $-3.8$  kcal/mol and  $-5.1$  kcal/mol, are likely to undergo oxidation more swiftly.

These data suggest that *B. paralicheniformis* cannot independently achieve full oxidation of all hydrocarbons and chemical derivatives in settings contaminated by crude oil.

## Abbreviations

Compilation of Polycyclic aromatic hydrocarbons (PAHs), A framework Data Files (SDF), Protein Data Bank (PDB). Tyrosine (TYR), Methionine (MET), Tryptophan (TRP), Isoleucine (ILE), Serine (SER), Alanine (ALA), Phenylalanine (PHE), Threonine (THR), Valine (VAL), Arginine (ARG), Proline (PRO), Glutamine (GLN), Leucine (LEU), Histidine (HIS), Asparagine (ASN), Glycine (GLY), Lysine (LYS).

## Conflicting interests

The authors assert that they possess no conflicting interests.

## Financial Support

No financial assistance, grants, or other help was obtained.

**Acknowledgements:** We acknowledge Vels Institute of Science, Technology and Advanced Studies (VISTAS) for so kindly facilitating the space and resources needed for research.

**Data availability declaration:** The relevant author kindly provides the data supporting the conclusions of this study upon appropriate request.



## REFERENCE

1. Ismila CI, Nor I, Nazliah MA, Ahmad I. A Study on preparedness and response of oil spill. J Phys: Conf Ser. 2020;1529:032088. <https://doi.org/10.1088/1742-6596/1529/3/032088>
2. Varjani SJ. Microbial degradation of petroleum hydrocarbons. Biores Technol. 2017;223:277-286. <https://doi.org/10.1016/j.biortech.2016.10.037>
3. Ajide OM, Isaac OO. An assessment of the physical impact of oil spillage using GIS and Remote Sensing technologies: Empirical evidence from Jesse town, Delta State, Nigeria. British J Arts and Soc Sci. 2013;12(2):235-252. [http://www.bjournal.co.uk/paper/BJASS\\_12\\_2/BJASS\\_12\\_02\\_08.pdf](http://www.bjournal.co.uk/paper/BJASS_12_2/BJASS_12_02_08.pdf)
4. Peterson CT, Grubbs RD, Mickle A. An investigation of effects of the deepwater horizon oil spill on coastal fishes in the Florida Big Bend using fishery-independent surveys and stable isotope analysis. Southeast Nat. 2017;16(1):93-108. <https://doi.org/10.1016/j.proeng.2018.01.136>
5. Pegg S, Zabbey N. Oil and water: the Bodo spills and the destruction of traditional livelihood structures in the Niger Delta. Community Dev J. 2013;48(3):391-405. <https://doi.org/10.1093/cdj/bsf021>
6. Dave D, Ghaly AE. Remediation technologies for marine oil spills: A critical review and comparative analysis. Am J Environ Sci. 2011;7(5):423-440. <https://doi.org/10.3844/ajessp.2011.423.440>
7. Xu X, Liu W, Tian S, et al. Petroleum hydrocarbon-degrading bacteria for the remediation of oil pollution under aerobic conditions: A perspective analysis. Front Microbiol. 2018;9:2885-2897. <https://doi.org/10.3389/fmicb.2018.02885>
8. Guerra AB, Oliveira JS, Silva-Portela RC, et al. Metagenome enrichment approach used for selection of oil-degrading bacteria consortia for drill cutting residue bioremediation. Environ Pollut. 2018;235:869-880. <https://doi.org/10.1016/j.envpol.2018.01.014>
9. Das N, Chandran P. Microbial degradation of petroleum hydrocarbon contaminants: An overview. Biotechnol Res Int. 2011;941810. <https://doi.org/10.4061/2011/941810>
10. Ikhajagbe B, Ogwu MC. Hazard quotient, microbial diversity, and plant composition of spent crude oil polluted soil. Beni-Suef Uni J Basic Appl Sci. 2020;9:26-35. <https://doi.org/10.1186/s43088-020-00052-0>
11. Chen W, Li J, Sun X, Min J, Hu X. High efficiency degradation of alkanes and crude oil by a salt-tolerant bacterium Dietzia species CN-3. Int Biodeterior Biodegrad. 2017;118:110-118. <https://doi.org/10.1016/j.ibiod.2017.01.029>
12. Fuentes S, Barra B, Caporaso JG, Seeger M. From rare to dominant: a fine-tuned soil bacterial bloom during petroleum hydrocarbon bioremediation. Appl Environ Microbiol. 2015;82: 888-896. <https://doi.org/10.1128/AEM.02625-15>
13. Tremblay J, Yergeau E, Fortin N, et al. Chemical dispersants enhance the activity of oil and gas condensate-degrading marine bacteria. ISME J. 2017;11:2793-2808. <https://doi.org/10.1038/ismej.2017.129>
14. Varjani SJ, Upasani VN. A new look on factors affecting microbial degradation of petroleum hydrocarbon pollutants. Int Biodeterior Biodegrad. 2017;120:71-83. <https://doi.org/10.1016/j.ibiod.2017.02.006>
15. Yang Y, Wang J, Liao J, Xie S, Huang Y. Abundance and diversity of soil petroleum hydrocarbon-degrading microbial communities in oil exploring areas. Appl Microbiol Biotechnol. 2015;99:1935-1946. <https://doi.org/10.1007/s00253-014-6074-z>
16. Das N, Chandra P. Microbial degradation of petroleum hydrocarbon contaminants: an overview. Biotech Res Int. 2011;941810: 1-13. <https://doi.org/10.4061/2011/941810>
17. Oyetibo GO, Chien MF, Ikeda-Ohtsubo W, et al. Biodegradation of crude oil and phenanthrene by heavy metal resistant *Bacillus subtilis* isolated from a multi-polluted industrial wastewater creek. Int Biodeterior Biodegrad. 2017;120:143-151. <https://doi.org/10.1016/j.ibiod.2017.02.021>
18. Okafor PC, Udemang NL, Chikere CB, Akaranta O, Ntushelo K. Indigenous microbial strains as bioresource for remediation of chronically polluted Niger Delta soils. Sci Afr. 2021;11:e00682. <https://doi.org/10.1016/j.sciaf.2020.e00682>
19. Pavlova A, Papazova D. Oil-Spill identification by gas chromatography-mass spectrometry. J Chromato Sci. 2004;41:271-273. <https://doi.org/10.1093/chromsci/41.5.271>
20. Driggers CM, Hartman SJ, Karplus PA. Structures of Arg- and Gln-type bacterial cysteine dioxygenase homologs. Protein Sci. 2015;24(1):154-161. <https://doi.org/10.1002/pro.2587>
21. Sasikala RP, Meena KS. Molecular docking studies and ADMET properties of compounds from *Physalis minima* L. leaves root and fruit. Innov J Life Sci. 2016;4:21-25. <https://innovareacademics.in/journals/index.php/ijls/article/view/11148>
22. Pettersen EF, Goddard TD, Huang CC, et al. UCSF Chimera- a visualization system for exploratory research and analysis. J Comput Chem. 2004;25(13):1605-1612. <https://doi.org/10.1002/jcc.20084>
23. Duru CE, Duru IA, Bilar A. Computational investigation of sugar fermentation inhibition by bergenin at the pyruvate decarboxylase isoenzyme 1 target of *Schistosoma mansoni*. J Med Plants Stud. 2020;8(6):21-25. <https://doi.org/10.22271/plants.2020.v8.i6a.1225>
24. BIOVIA DS. Discovery studio modeling environment. San Diego, Dassault Systemes, Release. 2020;20.1
25. Duru IA, Duru CE. Molecular docking of compounds in the essential oil of *Ocimum gratissimum* leaf against PIM-1 kinase of *Escherichia coli*. Euro J Adv Chem Res. 2020;1(6):14. <https://doi.org/10.24018/ejchem.2020.1.6.26>
26. Tsao YC, Chang YJ, Wang CH, Chen L. Discovery of isoplumbagin as a novel NQO1 substrate and anti-cancer quinone. Int J Mol Sci. 2020;21(12):4378. <https://doi.org/10.3390/ijms21124378>
27. Duru CE, Duru IA, Chidiebere CW. Virtual screening of selected natural products as human tyrosinase-related protein 1 blocker. J Nig Soc Phys Sci. 2021;3:154-158. <https://doi.org/10.46481/jnsps.2021.253>
28. Al-Karmalawy AA, Dahab MA, Metwally AM, et al. Molecular docking and dynamics simulation revealed the potential inhibitory activity of ACEIs against SARS-CoV-2 targeting the hACE2 receptor. Front Chem. 2021;9:661230. <https://doi.org/10.3389/fchem.2021.661230>
29. Rathoure AK (Ed.). Bioremediation: Current research and applications. I K International Publishing House Pvt. Ltd. New Delhi, India; 2017. p. 284-285. <https://www.ikbooks.com/books/book/earth-environmental-sciences/bioremediation/9789385909603/>